Antiproton-Yield and HBT Correlations

Sean Gavin and Claude Pruneau
Department of Physics and Astronomy
Wayne State University
Detroit, MI, 48202

We confront for the first time the widely-held belief that combined event-by-event information from quark gluon plasma signals can reduce the ambiguity of the individual signals. We illustrate specifically how the measured antiproton yield combined with the spacetime information from pion-pion HBT correlations can be used to identify novel event classes.

Antiproton production [1] and pion interferometry (HBT) [2] each provide independent measures of the spacetime evolution in relativistic heavy ion collisions. In both cases, however, this information has been difficult to extract from data owing to the complexity of nuclear-collision dynamics. Claude Pruneau and I propose that an event-by-event analysis combining antiproton yield measurements with radius parameters extracted from pion HBT can help to extract this spacetime information.

Of potentially greater importance, we suggest that antiproton-radius correlations can be used to identify novel event classes. Specifically, suppose that equilibrated continuous regions of quark-gluon plasma are produced only in a fraction of central collisions. While individual probes may prove ambiguous in this case, it has long been felt that event-by-event correlation of probes can identify anomalous event classes. However, not just any probes will do -- event-by-event measurements of bulk "thermodynamic" quantities, such as the average p_t, K/π and E_t, have been emphasized by CERN experiment NA49 [3]. NA49 results are consistent with a production mechanism that randomly populates phase space, e.g., freezeout from chemical and thermal equilibrium of pions and Kaons. While possibly useful for demonstrating equilibration in the hadronic matter, such quantities are useless in identifying novel events precisely because hadronic equilibration erases any novelty.

In this work we argue that the antiproton yield and pion HBT are not equilibrium quantities and therefore carry significant dynamical information that remains through freezeout. We point out for the first time the added information that can be obtained by measuring pion HBT and antiproton production simultaneously. To reach this goal we combine analytic calculations and numerical simulations. Next, we plan to develop the analysis tools needed to extract this information in the face of real event-by-event fluctuations – this will be done with RQMD and VNI simulations in the context of STAR. We stress that, whether or not novel event classes emerge, the experimental information on the baryon spacetime distribution can provide significant leverage in testing parton-cascade and hadronic models.

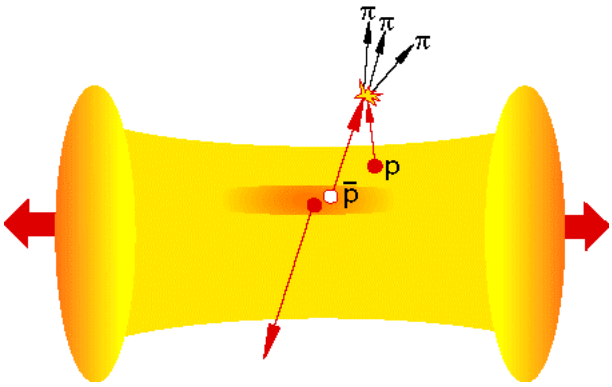

FIGURE 1: Artist's conception of antiproton production and annihilation.

Prior to the first AGS and SPS antiproton measurements, we had predicted that annihilation with baryons suppresses antiproton production [1]. Specifically, an increase in the spacetime extent of baryons of the collision system for a fixed initial baryon density leads to a decrease in the antiproton-to-proton ratio compared to that measured in proton-proton collisions. While suppression has been observed [4,5], the

$$R_p = \frac{\left(EdN/d^3p\right)_{\bar{p}}}{\left(EdN/d^3p\right)_p},$$

measured reduction at AGS energy is significantly smaller than calculations based on free-space antiproton production and annihilation cross sections. To remedy this disagreement, authors have introduced various effects such as screening [6,7], enhanced production [8] and additional antiprotons from strange antibaryon

decay together with enhanced strangeness [5]. At present, there is little objective information to indicate how much each effect contributes to antiproton production -- the spacetime information remains hidden.

It is well known that pion HBT bears implications about the spacetime history of high-energy collisions. Nuclear collision experiments demonstrate that an increase of the system's spatial size or lifetime is reflected in an increase the HBT radius parameters. These parameters are experimentally defined in terms of the pion correlation function,

$$C(K = p_1 + p_2, q = p_1 - p_2) = \frac{dN / d^3 p_1 d^3 p_2}{dN / d^3 p_1 ? dN / d^3 p_2} \sim 1 + \exp(-q_{\|}^{\ 2} R_{\|}^{\ 2} - q_o^{\ 2} R_o^{\ 2} - q_s^{\ 2} R_s^{\ 2}).$$

The longitudinal radius $R_{\|}$ and the difference between R_o and R_s are expected to increase the longer the bulk of the system remains near local thermal equilibrium. For the idealized case of Bjorken hydrodynamic evolution up to a well-defined freezeout time τ_F, the longitudinal radius satisfies

$$R_{\|}^{\ 2} \quad \frac{T}{\sqrt{m^2 + K^{\ 2}}} ¾\ \tau_F \sqrt[2]{\frac{}{\cosh y}}.$$

Approximate definitions of radius parameters applicable in an event-by-event setting are:

$$R_a^{\ -2} \qquad dq\, C(K,q)\, q_a^{\ 2} \Big/ \ dq\, C(K,q)\ ,|$$

where *a* refers to longitudinal, side or out radii.

Experiments NA44 and NA49 show dependence on kinematic variables similar to the above, despite the fact that flow and other dynamic effects complicate the extraction of direct spacetime information. Also, we point out that only a one-dimensional HBT analysis may be practical event-by-event. The corresponding one-dimensional radius reflects changes in τ_F, albeit less directly.

The yield of antiprotons in a nuclear collision depends on the spacetime evolution as follows. Antiproton production occurs as a soft hadronic process via string fragmentation. These antiprotons can then collide with any baryons and be annihilated. When the net baryon density is small compared to the densities of protons and antiprotons, as expected at RHIC, we relate the ratio R_p to its initial value $R_p^{\ 0}$ using:

$$R_p = R_p^{\ 0} S, \qquad \text{where} \qquad S = \exp\left(- \ d\tau\ n_B(\tau) \langle \sigma_a v_{rel} \rangle\right) \ (\tau_0 / \tau_F)^{\beta}.$$

Here, τ_0 is the antiproton formation time and τ_F is the freezeout time. The exponent β depends on the net density of comoving baryons $n_B(\tau)$, which satisfies:

$$\frac{dN_p}{dy} - \frac{dN_{\bar{p}}}{dy} \quad f\pi R^2 \tau_0 n_B^{\ 0},$$

where R is the nuclear radius and $f \sim 0.4$ is the fraction of antiprotons per baryon. Together with the equation for R_p, this equation determines the number of protons and antiprotons. Fluctuations in the net baryon number imply that

$$\beta = \langle \sigma_a v_{rel} \rangle \tau_0 \{ n_B^{\ 0} - \sigma_B^{\ 2} / 2 \};$$

the term proportional to n_B^0 is the average baryon density contribution from [1]. The variance term σ_B^2, which comes from averaging over Gaussian fluctuations in the net baryon number, is included because the net baryon density is small at RHIC. HIJING calculations show that this variance satisfies $\sigma_B^2 \sim n_B$ and can be large.

The exponent also depends on σ_a the energy-dependent annihilation cross section and v_{rel} the relative velocity, with the collision frequency per unit volume

$$\langle \sigma_a v_{rel} \rangle = \frac{1}{n\bar{n}} \int \frac{d^3p_1}{(2\pi)^3} \frac{d^3p_1}{(2\pi)^3} f(p_1)\bar{f}(p_2)\sigma_a v_{rel}.$$

In [1] we obtain a value ~44 mb by using an empirical parameterization of the annihilation cross section and taking baryon and antibaryon distributions to be thermal at temperature T~170 MeV.

Beyond the hadronic framework applicable at AGS/CERN energies, both antiproton and two-pion HBT distributions can vary from our hadronic expectations if quark gluon plasma forms. A variety of mechanisms from chiral restoration to disoriented chiral condensate formation [9,10,11] can enhance production of baryon-antibaryon pairs. Model calculations typically yield values of the antiproton *dN/dy* approaching values well in excess of event generators. For example, if the entire collision volume is converted to chemically-equilibrated quark-gluon plasma, then

$$\left(dN_{\bar{p}}/dy\right)_{QGP} \quad 40$$

In comparison, HIJING, HIJING/BBbar (its successor) and RQMD give values of 30, 10 and 10 respectively.

For HBT, Pratt and Bertsch [2] have argued that plasma formation can increase the pion HBT radius parameters, e.g., if a nearly-first-order phase transformation leads to the dramatic increase of the collision-system lifetime and size. The increase in the lifetime of the plasma system can be dramatic - if the expanding plasma region reaches T_c at a time 1 fm, then hadronization can take as much as 37/3 fm (the ratio of the number of degrees of freedom in plasma and hadron gas). If seen, a trend with larger systems producing more antiprotons and protons runs counter to hadronic expectations.

To estimate the hadronic correlations between HBT radii and antiproton production, we performed the following calculations. We take the initial production of protons and antiprotons in a central collision to yield rapidity densities of 22.5 and 20, respectively. These values are midway between HIJING and HIJING/BBbar (observe that these codes do not include annihilation, or any final state interactions). We assume these rapidity densities are proportional to the number of participants, $\nu(b)$, and use the wounded nucleon model to estimate the dependence on impact parameter, b (this agrees with full HIJING calculations at the 1-2 percent level). We assume the freezeout time to grow as $\nu(b)^{1/3}$ to a value $\tau_F(b=0) \sim$ 17.5 fm, in rough accord with simulations of Gavin, Bellwied and Humanic [13]. The Makhlin-Sinukov formula gives a value of the longitudinal radius of ~ 12.5 fm, in good agreement with RQMD calculations of Hardtke [12]. We then take $\tau_0 \sim 1$ fm and estimate the effect of absorption following [1].

We developed a Monte Carlo event generator to exhibit the event-by-event distribution of the mean number of antiprotons in the STAR acceptance as well as the HBT radius. Fluctuations in the antiproton yield are Gaussian with a variance ~N, in accord with HIJING simulations. Fluctuations in the HBT longitudinal radius are distributed with $\Delta R/R \sim 10\%$. This width describes the effect of event-by-event fluctuations in collision geometry and freezeout time on the longitudinal radius. Pandey [14] used RQMD with Pratt's

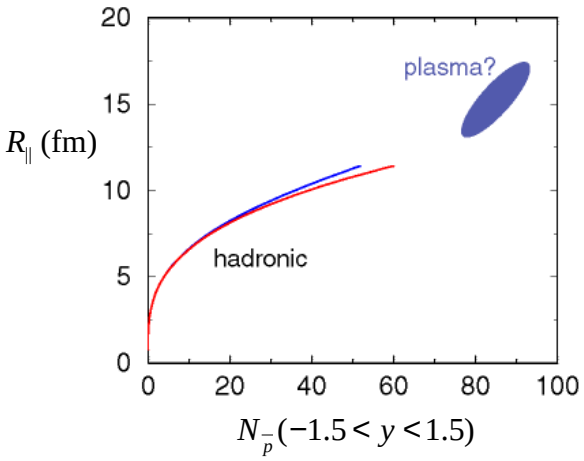

FIGURE 2. The hadronic trend in longitudinal radius and antiproton multiplicity. The correlation in the upper curve shows the correlation from centrality alone, while the lower curve includes annihilation. The plasma exhibits qualitatively different behavior.

CRAB afterburner to study the uncertainty in extracting the invariant R by fitting the event-by-event correlation function with a Gaussian. While these fluctuations are up to three times larger at the largest R, the integral approximation to R suggested above may reduce fluctuations.

To develop a procedure for bringing out new event classes, we explore a conservative scenario for plasma formation at RHIC in which we assume that plasma forms in nearly central collisions and only in a fraction of events

$$f = 0.25\,(1 - b^2 / b_0^{\,2}), \qquad \text{for } b < b_0 \quad 3\,\text{fm}.$$

In these events, we then assume that only the innermost 1/3 of the collision volume turns into plasma. The net enhancement of the number of initial antiprotons is fixed by the plasma chemical-equilibrium value above, but this huge enhancement is diluted because only 1/3 of the volume participates. The combined hadronic plus plasma signal for antiproton production is shown in figure 3 for 10,000 events.

The distribution of individual Monte Carlo events versus impact parameter is shown in figure 4. The antiproton signal remains unpersuasive but the HBT events perhaps show a separate class of events at low b. We take the freezeout time and, consequently, the longitudinal radius to increase by a factor ~ 1.5 in the plasma events, so that $\tau_F(b=0) \sim 25$ fm for plasma events. We point out that recent calculations from Bass et al. for hydrodynamic quark-gluon plasma evolution followed by UrQMD kinetics suggest a similar mean lifetime for plasma events, ~ 23.1 fm/c [15].

The correlated signal is shown in fig. 5. Here, two event classes are clearly separated. We now identify the events with the largest antiproton yield as anomalous. One can then introduce an antiproton trigger to create a large sample of anomalous events for further statistical analysis.

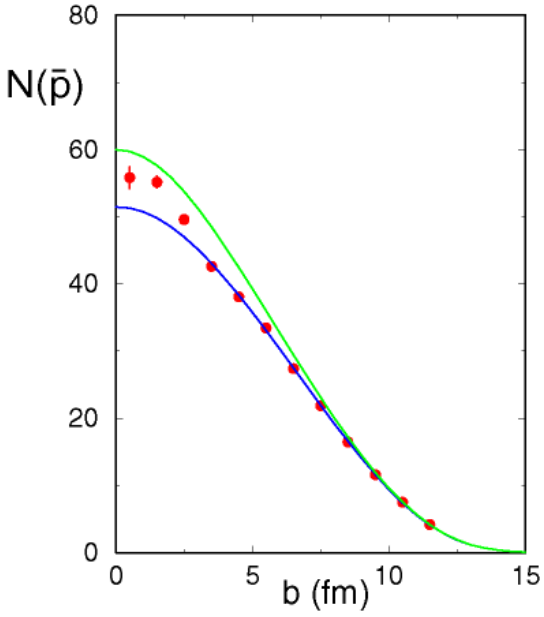

FIGURE 3. Combined plasma-enhancement and annihilation in 10,000 Monte Carlo events (points). The curves show hadronic production (upper curve) and annihilation (lower). The effect of plasma in the Monte Carlo simulations is the increase at small *b*.

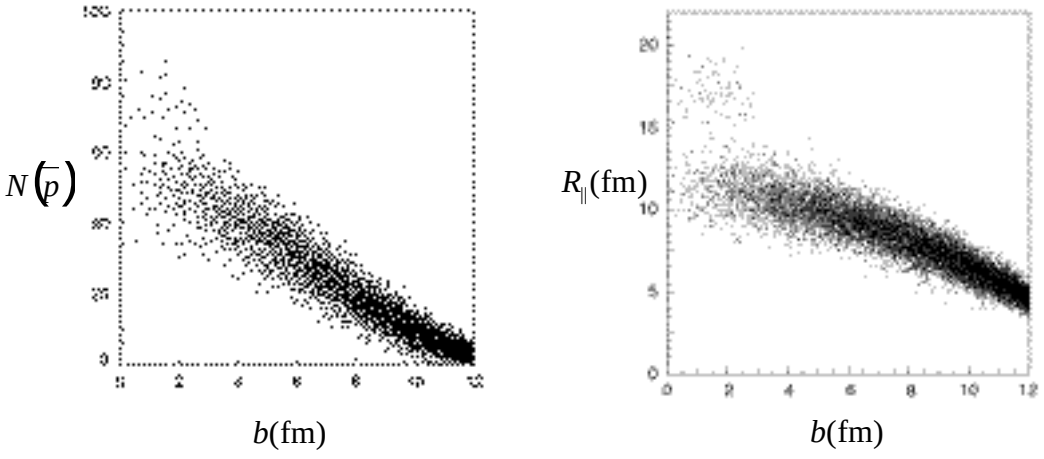

FIGURE 4. Distribution of Monte Carlo events with impact parameter.

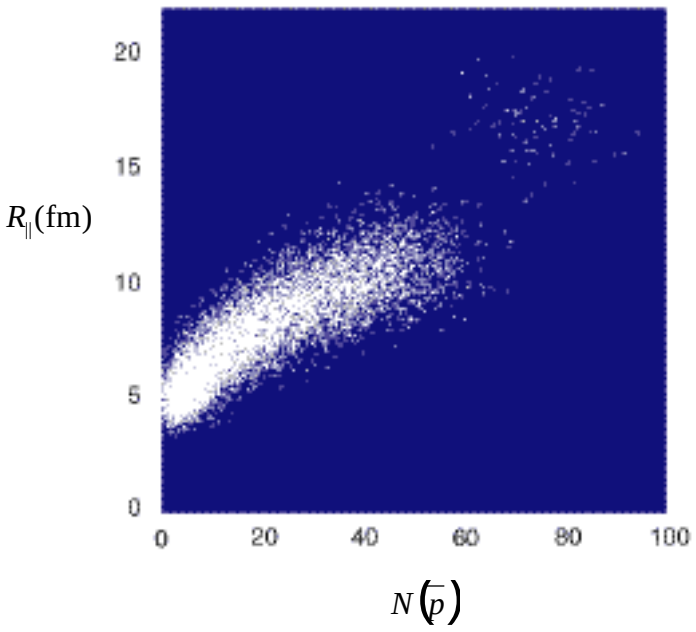

FIGURE 5. Correlated antiproton yield and HBT radius shows two event classes.

We are currently extending this study to one-dimensional HBT parameters. So far we have emphasized the longitudinal radius, because $R_{\|}$ is proportional to the freezeout time for the case of Bjorken flow. However, it is important to realize that more experimentally accessible one-dimensional HBT variables like the transverse radius R_T are also positively correlated with the event lifetime. R_T is strongly correlated to τ_F because a system must remain in local equilibrium longer for it to reach a larger transverse radius. Flow enhances this positive correlation. We therefore expect a similar correlation of R_T with the antiproton yield, even though R_T does not "measure" τ_F. While three-dimensional analyses might prove impractical on an event-by-event basis, STAR collaborators expect one-dimensional HBT analyses to provide useful information [14].

It will eventually be necessary to use models like RQMD and VNI to study correlated observables. However, it is not clear that the dynamical correlations these models produce are realistic, since they are only tuned to fit single-particle data. On the experimental side, we plan to work with Pandey [14] to determine how to extract event-by-event in HBT radii in practice. If experimental fluctuations in HBT radii are too large, it will be necessary to develop a super-event analysis [16] scheme as in Gavin, Greene and Miller [17] to pick out finer detail in the correlated behavior.

[1] S. Gavin, M. Gyulassy, M. Plümer and Venugopalan, Phys. Lett. **234B**, 175 (1990).

[2] See e.g. S. Pratt, Nucl. Phys. **A638**, 125c (1998); Phys. Rev. **D33** 1314 (1986).

[3] G. Roland, Nucl. Phys. **A638**, 125c (1998).

[4] M. J. Bennett et al. (E878 Collab.) Phys. Rev. **C56** 1521, (1997); Y. Akiba et al. (E866 Collab.), Nucl. Phys. **A610**, 139c, (1996).

[5] T. A. Armstrong et al. (E864 Collab.) Phys. Rev. Lett. **79**, 3351 (1997); J. Nagle, Yale University Ph. D. thesis (1997); B. A. Cole, private communications.

[6] A. Jahns, H. Stoecker, W. Greiner and H. Sorge, Phys. Rev. Lett. **68** 2895, (1992); A. Jahns, C. Spieles, R. Mattiello, H. Stoecker, W. Greiner and H. Sorge, Phys. Lett. B308 11, (1993); Erratum-ibid. B314, 482, (1993).

[7] S. H. Kahana, Y. Pang, T. Schlagel, C. B. Dover, Phys. Rev. **C47** 1356, (1993); Y. Pang, D.E. Kahana, S.H. Kahana, H. Crawford, Phys. Rev. Lett. **78**, 3418 (1997).

[8] C. Spieles, et al., Phys. Rev. **C53**, 2011 (1996).

[9] T. A. DeGrand, Phys. Rev. **D30** 2001, (1984).

[10] U. Heinz, P.R. Subramanian, W. Greiner, Z. Phys. **A318**, 247 (1984); P. Koch, B. Müller, H. Stocker and W. Greiner, Mod. Phys. Lett. **A3**, 737 (1988).

[11] J. Ellis, U. Heinz and H. Kowalski, Phys. Lett. **B233**, 223 (1989); J. I. Kapusta and A. M. Srivastava, Phys. Rev. **D52**, 2977 (1995).

[12] D. Hardtke, STAR Note 384.

[13] R. Bellwied, S. Gavin and T. Humanic, nucl-th/9811085.

[14] S. Pandey, SVT Proposal; private communication.

[15] S. A. Bass et al., nucl-th/9902062.

[16] J. Sandweiss, private communication.

[17] S. Gavin, S. V. Greene, T. Miller, in progress.